Arch Pharm Res Vol 32, No 7, 1077-1086, 2009
DOI 10.1007/s12272-009-1714-z

Archives of Pharmacal Research
www.springer.com/12272

Suppression of Hepatitis B Virus-derived Human Hepatocellular Carcinoma by NF-κB-inducing Kinase-specific siRNA using Liver-Targeting Liposomes

Hyun-Ah Cho[1], In-Sung Park[1], Tae-Woo Kim[2], Yu-Kyoung Oh[3], Ki-Sook Yang[1], and Jin-Seok Kim[1,4]

[1]College of Pharmacy, Sookmyung Women's University, Seoul 140-742, Korea, [2]Laboratory of Infection and Immunology, Korea University of Medicine, Seoul 136-701, Korea, and [3]School of Life Science and Biotechnology, Korea University, Seoul 136-701, Korea

(Received March 11, 2009/Revised June 24, 2009/Accepted July 7, 2009)

Hepatitis B virus triggers an increase of NF-κB inducing kinase (NIK)-dependent NF-κB activation, followed by the promotion of hepatocellular carcinoma (HCC). Here, we examined the inhibitory effect of NIK-specific siRNA on NF-κB signaling and HCC. The results of this study indicated that these siRNAs suppressed HBV-derived HCC by regulating NIK activation. To exert a protective effect from degradation enzyme, cationic liposomes were contrived and modified to contain β-sitosterol glucoside to target the asialoglycoprotein receptors in liver cancer cells. The cationic dimyristoyl diacyltrimethylammonium propane liposomes were prepared by a reverse-phase evaporation method with slight modification. β-Sitosterol glucoside was added to the lipid mixture at the beginning of the liposome preparation for the purpose of liver targeting. These liposomes assisted the delivery of the siRNA to specific cells and protected it from various lyases, followed by the ultimate suppression of HCC.

Key words: siRNA, DMTAP, Beta-sitosterol glucoside, Liposomes, Hepatitis B Virus, NF-κB-inducing kinase

INTRODUCTION

Human hepatitis B virus (HBV) is known to cause acute and chronic infections in the human liver. By inducing changes in various intracellular signal transductions (Rabe et al., 2001), chronic HBV infection leads to severe liver diseases such as liver fibrosis, cirrhosis and even hepatocellular carcinoma (Ryu et al., 2006). HBV is particularly known to trigger the activation of NIK-dependent NF-κB; this NF-κB signaling pathway is an important regulator in liver disease. As a result of HBV infection, NF-κB promotes HCC by preferentially keeping the transformed hepatocytes alive over normal hepatocytes in the inflamed tissue (Mann and Oakley, 2005). The transcription factor NF-κB regulates the balance between proliferation and apoptosis toward malignant growth in tumor cells (Rabe et al., 2001). NF-κB represents a family of eukaryotic transcription factors that participate in regulating the immune response, cell growth and survival. In most cells, NF-κB is restricted to the cytoplasm by the inhibitory protein IκB. IκB becomes phosphorylated by the IκB kinase (IKK) complex, which leads to its degradation and the liberation of NF-κB for nuclear translocation (Ghosh and Karin, 2002). The IKK complex is composed of two catalytic subunits, IKKα and IKKβ, as well as a regulatory subunit, IKKγ (Zandi et al., 1997). The kinase activities of both IKKα and IKKβ are induced by a wide variety of NF-κB inducers, which are upstream kinases that include the NF-κB-inducing kinase (NIK) (Okamoto et al., 1997).

NIK was first identified on the basis of its association with TNF-receptor-associated factor 2 (TRAF2). NIK associates with the phosphorylation of IKKα and IKKβ (Malinin et al., 1997). When overexpressed, NIK enhances NF-κB activity and the expression of kinase-defective NIK blocks NF-κB activation in response to most inducers (Richmond, 2002). RNA interference

Correspondence to: Jin-Seok Kim, College of Pharmacy, Sookmyung Women's University, Seoul 140-742, Korea
Tel: 82-2-710-9574, Fax: 82-2-712-0032
E-mail: jsk9574@sm.ac.kr

(RNAi) is a potent gene silencing mechanism conserved in all mammals (Nakano et al., 1998; Hannon, 2002; Dykxhoorn et al., 2003). Gene-specific double-stranded RNA (dsRNA) knocks down gene expression at the level of messenger RNA through the gene silencing mechanism (Kittler and Buchholz, 2003). Long dsRNA molecules are processed to small 21- to 23-nucleotide interfering RNAs by Dicer, an endogenous RNAIII enzyme. These small interfering RNAs (siRNA) were first discovered in plants exhibiting transgene-mediated RNA silencing, and are believed to guide the RNA interfering silencing complex (RISC). RISC contains the proteins necessary to unwind double-stranded siRNAs and to cleave the target mRNAs at the site of antisense RNA binding (Sharp, 2001). In mammalian cells, long dsRNA triggers the interferon responses that are thought to be mediated in part by the activation of PKR, a kinase activated by dimerization in the presence of dsRNA. PKR phosphorylates and inactivates the inhibition of protein synthesis. This process has emerged as an effective means of selectively silencing gene expression in mammalian cells (Stark et al., 1998, Elbashir et al., 2001, Sorensen et al., 2003).

Current treatment strategies for HCC that originates from HBV infection are limited because of low drug efficacy and the emergence of drug-resistant mutants. Recent reports have shown that siRNA can be used a novel therapeutic strategy to treat HBV-derived HCC. In order to effectively deliver siRNAs into hepatocytes to treat HBV infection, drug delivery systems such as liposomes, with the capacity to target the liver are ideal. Cationic liposomes, formulated with cationic lipids based on diacyltrimethylammonium propane (dioleoyl-, dimyristoyl-, disteroyl-: DOTAP, DMTAP, DSTAP), have been accepted for siRNA delivery (Qi et al., 2005, Zhang et al., 2007).

The results of the present study show that suppression of NIK activity using siRNA reduced the proliferation of HCC that originated from HBV infection. This inhibition was associated with the nuclear localization of NIK, a novel mechanism of NF-κB activation. The inhibition of NIK by siRNA is expected to play a significant role in preventing HCC development from HBV infection. We evaluated the toxicity and efficacy of the delivery of liposomes formulated with various cationic lipids and then selected the DMTAP liposomes for further use. SG, derived from *Hibiscus manihot,* is known to accumulate in the liver, especially in hepatocytes (Kawano et al., 2002). Hence for the purpose of liver targeting, SG was conjugated with the liposomes to deliver the siRNA to the asialoglycoprotein receptors (ASGPR) in the hepatocytes.

MATERIALS AND METHODS

Reagents

Fetal bovine serum (FBS), penicillin-streptomycin, Dulbecco's Modified Eagle's Medium (DMEM), and RPMI 1640 were purchased from WelGENE Inc. (Daegu, Korea). Three different kinds of siRNAs (1180, 1269 and 1397) corresponding to the NIK gene were synthesized by Invitrogen (Carlsbad, CA). Dioleoylphosphatidylethanolamine (DOPE), dioleoyl diacyltrimethylammonium propane (DOTAP), dimyristoyl diacyltrimethylammonium propane (DMTAP), and disteroyl diacyltrimethylammonium propane (DSTAP) were purchased from Avanti Polar Lipids (Alabaster, AL). Sephadex G-50 column, RNase A, and 3-(4,5-dimethyl-2-thiazolyl)-2,5-diphenyl-2H-tetrazolium bromide (MTT) were from Sigma Chemicals (St. Louis, MO). Luciferase assay kit was purchased from Promega Corp. (Madison, WI). pNF-κB-luciferase was kindly provided by Prof. GH Jung (Seoul National University, Seoul, Korea). *Hibiscus manihot*-derived SG was supplied by Prof. KS Yang (Sookmyung Women's University, Seoul, Korea). Lipofectamine™ 2000 transfection reagent, RT-PCR Kit, GAPDH forward and reverse primers, NIK forward and reverse primers, and *Taq* polymerase were purchased from Invitrogen (Carlsbad, CA). HBsAg ELISA kit was purchased from Koma Biotech (Seoul, Korea). All other reagents were of analytical grade.

Preparation of siRNAs

Three different siRNAs (1180, 1269 and 1397) corresponding to the NIK gene were synthesized by Invitrogen as follows: siRNA 1180, Sense primer UCC AGU GGA CCU CUU CUC GAU ACU C, Antisense primer GAG UAU CGA GAA GAG GUC CAC UGG A; siRNA 1269, Sense primer UUU GAC AGC CAC CUG GAA GCC UGU C, Antisense primer GAC AGG CUU CCA GUG UGC UGU CAA A; siRNA 1397, Sense primer AGC AGU UCC AUG AAG AUG UUC ACC C, Antisense primer GGG UGA ACA UCU UCA UGG AAC UGC U.

Preparation of liposomes

The DOTAP liposome was prepared using a mixture of DOTAP and DOPE by the reverse-phase evaporation vesicle (REV) method with a slight modification. Briefly, DOTAP:DOPE (molar ratio of 1:1) was dissolved in chloroform (1 mL). After evaporation of the solvent under nitrogen gas at room temperature, the lipid residue was placed on a vacuum pump for 10-15 min to remove any residual organic solvent. The dry lipid film was suspended in distilled water at twice

the final lipid concentration and the solution was sonicated for 3 min. An equal volume of HEPES buffer (pH 7.4) was added and sonicated for 2 min. Cationic liposomes were prepared using a mixture of cholesterol and DMTAP or DSTAP by the REV method. Lipids (1:1 molar ratio) were dissolved in chloroform (1 mL) and the solvent was evaporated under nitrogen gas at room temperature. After that, the dry film was suspended in 1 mL of freshly hydrated diethyl ether, to which 1 mL of HEPES buffer (pH 7.4) was added. The mixture was vigorously vortexed for 1 min and was sonicated for 3 min. Ether was then removed by rotary evaporation. Liposomes were separated from the lipid residue by gel chromatography using a Sephadex G-50 column. Liposomes were downsized by extrusion through 0.4- and 0.2-μm polycarbonate membranes 10 to 20 times using a Liposofast™ extrusion device (Avestin, Toronto, Canada). SG was added to the lipid mixture at the beginning of the liposome preparation for SG-containing liposomes. The entire extruder was autoclaved prior to use and all reagents and glassware used for liposome preparation were also sterilized.

Cell culture

HepG2 and HepG2.2.15 cells were cultured in DMEM in the presence of 10% fetal bovine serum and 150 μg/mL penicillin-streptomycin under 5% CO_2 at 37°C. A549 cells were cultured in RPMI 1640 in the presence of 10% fetal bovine serum and 150 μg/mL penicillin-streptomycin under 5% CO_2 at 37°C.

Transfection

To dilute DNA or siRNAs, 4 μg DNA or 100 pM siRNAs were added to 250 μL of serum-free media. Ten μL of Lipofectamine™ 2000 was diluted in 250 μL of serum-free media. After 5 min of incubation at room temperature, the solutions were mixed gently with each other and incubated for another 20 min at room temperature. The resulting complexes were added to each well of 6-well plates containing cells.

Cell viability test

The relative number of viable cells after siRNA treatment was obtained from MTT assays. Briefly, 0.4×10^5 A549 cells per well, 0.6×10^5 HepG2 cells per well, and 0.6×10^5 HepG2.2.15 cells per well were plated on 24-well plates and incubated overnight. After incubation for 24 h with siRNAs, viability was determined by addition of 10 μL of MTT stock solution (10 mg/mL in PBS) to each well. After incubation for 3-4 h at 37°C, the medium and MTT were removed, and then 100 μL of DMSO was added to dissolve the formed formazan crystals. Absorbance was measured at 570 nm with a microplate reader. All measurements were done in triplicate.

Reporter gene assay

pNF-κB-luciferase reporter activity was determined in 6-well dishes seeded at a density of 1.5×10^5 A549 cells per well and 2.5×10^5 HepG2 or HepG2.2.15 cells per well. Following 24 h of growth, the cells were transfected with 4 μg of pNF-κB-luciferase and 100 pM of siRNAs using lipofectamine™ 2000 transfection reagent according to the manufacturer's protocol. After 24 h, the cells were lysed and luciferase activity was measured using a luciferase assay kit according to the manufacturer's protocol.

Reverse transcription-polymerase chain reaction (RT-PCR)

Cells were transfected with siRNAs and incubated overnight. Total RNA was isolated using TRIzol reagent according to the manufacturer's protocol (Invitrogen). cDNA was synthesized from the isolated total RNA by incubation for 30 min at 55°C. Following reverse transcription, the synthesized cDNA was amplified with *Taq* polymerase (Invitrogen). The primer sequences were as follows: GAPDH specific forward 5'-CTCAGACACCATGGGGAAGG-3', GAPDH specific reverse 5'-GTGGCAGTGATGGCATGGA-3', NIK specific forward 5'-TACGCCACTCACGAAGGAT-3', NIK specific reverse 5'-CAAGGGAGGAGACTT-GTTTG-3'. GAPDH PCR amplification was performed using a RT-PCR system (Invitrogen) with 2 min initial denaturation at 94°C and 40 cycles of 15 sec at 94°C, 30 sec at 60°C and 1 min at 68°C, followed by 5 min of extension at 68°C. NIK PCR amplification was performed using RT-PCR system with 5 min initial denaturation at 95°C and 35 cycles of 50 sec at 95°C, 50 sec at 60°C and 50 sec at 72°C, followed by 7 min of extension at 72°C. The PCR fragments were separated electrophoretically in 1% agarose gel.

HBsAg enzyme-linked immunosorbent assay

The expression levels of HBsAg were detected using an HBsAg ELISA kit (Koma Biotech). Positive and negative controls (100 μL) as well as the test samples were dispensed into each well, and 25 μL of detection antibody was cautiously dispensed into each well, except for the substrate blank. After that, the plate was gently shaken for mixing purposes and then incubated at 37°C for 90 min. After the liquid was aspirated from the wells and the plate was washed five times with 300 μL of wash buffer per well, 100 μL of color development solution was added at room

temperature and then incubated for 30 min. The absorbance of the plate was then read at a wavelength of 450 nm.

Size distribution analysis

The mean diameter and zeta-potential of the liposomes were determined by dynamic laser-light scattering (Particle Sizing System, Inc.) at room temperature using a He-Ne laser light source.

Transmission electron micrograph (TEM)

Liposomes were allowed to settle on glow-discharged carbon-coated grids, blot-dried, and stained with 2% uranyl acetate. The grids were examined using a transmission electron microscope (Tecnai 12, Philips, Eindhoven).

RNase A assay

Degradation of siRNA was observed using the RNase A assay. Liposomes were mixed with siRNA and incubated for 20 min. The siRNA-containing liposomes were mixed with 0.01 mg/mL of RNase A. After 0, 15, 30, 45 and 60 min, the liposomes were broken by sonication in a bath-type sonicator (Laboratory Supplies Co. Inc.) and degradation of siRNA was observed.

Fluorescence microscopic study

The cells, 2.5×10^5 HepG2.2.15 cells per well were plated on 6-well plates. After incubation for 24 h, Block-It™ fluorescent oligo (Invitrogen) encapsulated in SG-DMTAP liposome was transfected in cells. Fluorescence was detected using an inverted research microscope (IX71IX51, Olympus).

GUAVA ExpressPlus assay

Block-It™ fluorescent oligo encapsulated in SG-DMTAP liposome was transfected in cells, and the cells were harvested and suspended by PBS buffer. Transfection efficiency was detected by the manufacturer's protocol (GUAVA, GE Healthcare Bio-Sciences, Little Chalfont). The ExpressPlus data for all samples within was analyzed immediately after the sample is acquired using CytoSoft software.

Liposome encapsulation efficiency study

The siRNA-containing SG-DMTAP liposome was treated by 0.5% sodium dodecyl sulphate (SDS) for 10 min to promote lysis of the liposome, and siRNA was released from the lysed liposome. The amount of siRNA was spectrophotometrically determined at 280 nm. The encapsulation efficiency was expressed as the percentage of the total amount of siRNA that became encapsulated.

RESULTS

Cell viability and cytotoxicity

To confirm the therapeutic efficacy of HBV-specific siRNAs in HBV-derived HCC cells, a cell viability test was performed. According to the nuclear factor-κB (NF-κB) signaling pathway, NIK can enhance NF-κB activity. Thus, suppression of NIK would limit the activity of NF-κB. Suppression of NIK activity by NIK-specific siRNAs designed to reduce the level of NIK was expected to inhibit both endogenous and transfected NF-κB. As a result, these suppressions would inhibit HBV-derived hepatocellular carcinoma cell proliferation. To study the inhibitory activity of these siRNAs, pNF-κB-luciferase was transfected into HepG2.2.15 cells, a derivative of the human HepG2 hepatoma cells, by a stable transformation with several copies of the HBV genome. As shown in Fig. 1A, all three siRNAs (1180, 1269, and 1397) inhibited the viability of HepG2.2.15 cells by about 30% based on the results of MTT assays. However, through Figs. 2A, 3A, and 3B, siRNA 1397 was chosen as the most outstanding siRNA to inhibit HBV-derived HCC cells and replication of HBV in HepG2.2.15 cells among the three designed siRNAs.

siRNA is very unstable in serum and does not possess long-lasting stability. Fig. 1B shows that naked siRNA inhibited cell viability by about 15% in HepG2.2.15 cells after 24 h. The siRNA degraded rapidly in 1 h, as shown by the slope of the viability-time curve. To delay the clearance of siRNA from lyases, cationic liposomes were adopted. siRNA 1397 was encapsulated in various cationic liposomes with different phospholipids of DOTAP, DMTAP, or DSTAP, and Lipofectamine™ 2000 was used as a control. Encapsulated siRNA in the designed cationic liposomes continuously suppressed cell viability. The efficacy of siRNA encapsulated in the DOTAP liposome was the most significant in HepG2.2.15. The rank order of the suppression of the cell viability was DOTAP °Ð DMTAP > DSTAP liposome. HepG2.2.15 cell viability was inhibited by about 42% by DOTAP and DMTAP liposomes.

Cytotoxicity was confirmed in HepG2.2.15 cells (Fig. 1C). Although DOTAP liposomes showed the most significant efficacy in HepG2.2.15 cells (Fig. 1B), DMTAP was chosen as the most suitable carrier due to the relatively high toxicity of DOTAP. DMTAP significantly suppressed proliferation of HepG2.2.15 cells with a relatively low toxicity of 13% (Fig. 1C) and proved to be the most suitable as shown in Fig. 4. Fig. 1D shows the protective effects and specificity of

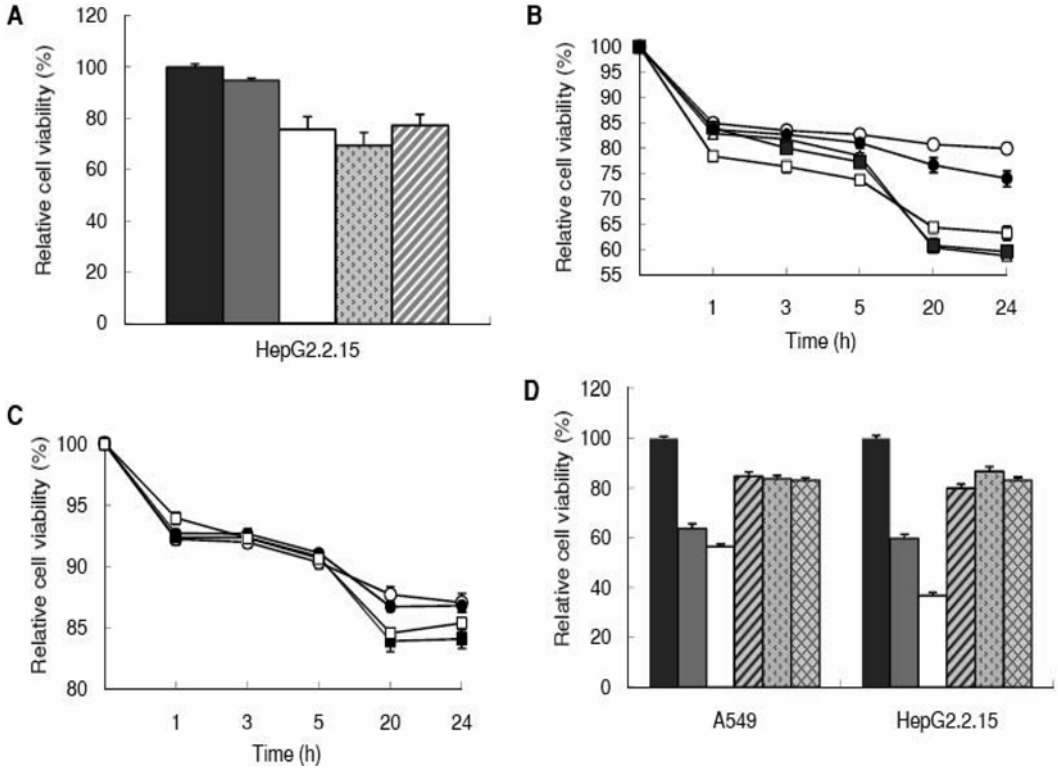

Fig. 1. A, Cell viability assay using the HepG2.2.15 cells after treatment with three different siRNAs. ■ pNF-κB-luciferase ■ pNF-κB-luciferase + scrambled siRNA □ pNF-κB-luciferase + siRNA 1180 ▨ pNF-κB-luciferase+siRNA 1269 ▨ pNF-κB-luciferase + siRNA 1397. **B**, Protection of siRNAs from degradation by various liposomes. —○— siRNA only —□— siRNA+lipofectamine™ 2000 —△— siRNA+DOTAP —■— siRNA + DMTAP —●— siRNA+DSTAP; To observe the protective effect of three different cationic liposomes (DOTAP, DMTAP, and DSTAP liposomes). Cell viability was measured by MTT assays of HepG2.2.15 cells in medium with serum after 0, 1, 3, 5, 20, or 24 h. siRNA 1397 was encapsulated in three different cationic liposomes, and lipofectamine™2000 was used as a control. **C**, Cytotoxicity of various liposomes in HepG2.2.15. —○— Lipdfectamine™ 2000 —■— DOTAP —●— DMTAP —□— DSTAP; To observe the cytotoxicity of three different cationic liposomes (DOTAP, DMTAP, and DSTAP) in HepG2.2.15, cell viability was measured by the same protocol used in (**B**). **D**, Liver targeting of the liposomes by SG. ■ pNF-κB-luciferase ■ pNF-κB-luciferase + DMTAP/siRNA □ pNF-κB-luciferase + SG-DMTAP/siRNA ▨ pNF-κB-luciferase + lipofectamine™ 2000/siRNA ▨ pNF-κB-luciferase + DMTAP ▨ pNF-κB-luciferase + SG-DMTAP; Cell viability of HepG2.2.15 cells was measured by MTT assay following treatment with siRNA 1397 encapsulated in liposomes.

DMTAP and SG-DMTAP liposomes for HepG2.2.15 cells that are known to express ASGPR. A549 cells do not express ASGPR and were therefore used as a negative control. A549 cells were used to compare the specific effects of DMTAP liposome modified with SG in liver cancer cells that have ASGPR (HepG2.2.15) and in cells that do not contain this receptor (A549). MTT assays using HepG2.2.15 and A549 cells revealed that naked siRNA inhibited the viability of A549 and HepG2.2.15 cells by about 15%. On the other hand, DMTAP liposome-encapsulated siRNA inhibited viability of both cells by about 40%. Furthermore, SG-DMTAP liposomes-encapsulated siRNA inhibited viability of HepG2.2.15 cells by about 62%. Thus, SG brought 20% specificity to the DMTAP liposome.

Suppression of NF-κB expression

To confirm the suppression of the expression levels of NF-κB in HepG2.2.15 cells by the three designed siRNAs through the reduction of NIK levels, the cells were transfected with pNF-κB-luciferase. Transfection of pNF-κB-luciferase allowed for the detection of NF-κB expression after siRNA treatment by luciferase light emission. Fig. 2A shows that the expression level of NF-κB was reduced by approximately 30% by all three designed siRNAs in their naked form. Suppression of the expression level of NF-κB by liposome-encapsulated siRNA1397 was also tested in pNF-κB-luciferase-transfected HepG2.2.15 cells. As shown in Fig. 2B, SG-containing DMTAP liposomes proved to be the most optimum in this regard, exhibiting an additional 20% suppression of NF-κB expression levels. Thus, SG afforded about 20% specificity to the

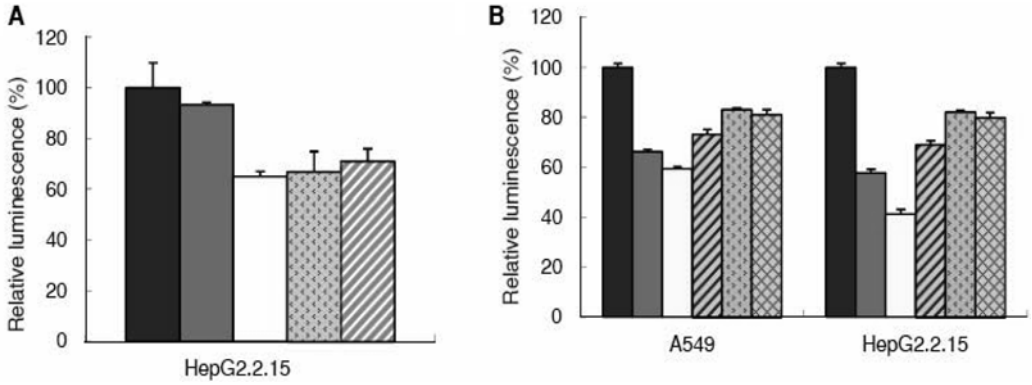

Fig. 2. A, Inhibition of NF-κB activity in HepG2.2.15 cells after pNF-κB-luciferase transfection by treatment with three siRNAs. ■ pNF-κB-luciferase ■ pNF-κB-luciferase + scrambled siRNA □ pNF-κB-luciferase + siRNA 1180 ▨ pNF-κB-luciferase + siRNA 1269 ▨ pNF-κB-luciferase + siRNA 1397. **B**, Inhibition of NF-κB activity in HepG2.2.15 and A549 cells after pNF-κB-luciferase transfection by siRNA 1397 encapsulated in various liposomal formulations. ■ pNF-κB-luciferase ■ pNF-κB-luciferase + DMTAP/siRNA □ pNF-κB-luciferase + SG-DMTAP/siRNA ▨ pNF-κB-luciferase + lipofectamine™ 2000/siRNA ▨ pNF-κB-luciferase + DMTAP ▨ pNF-κB-luciferase + SG-DMTAP.

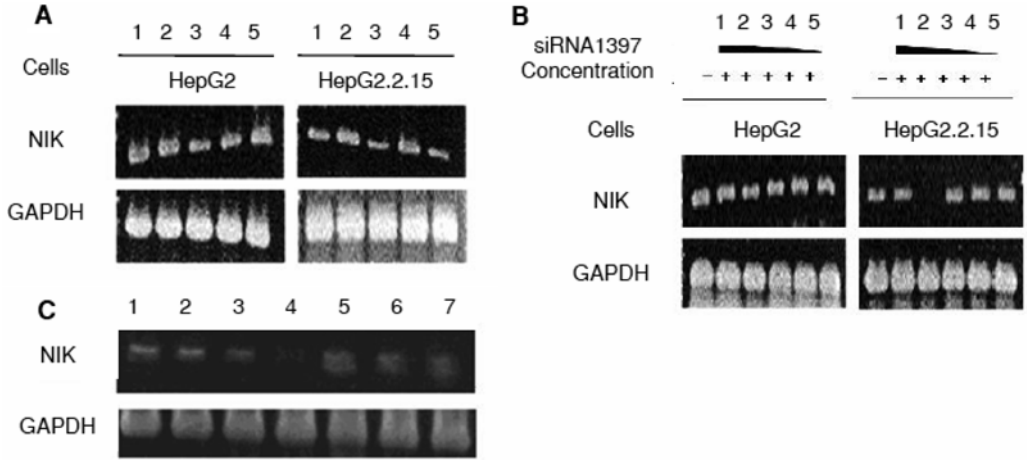

Fig. 3. A, RT-PCR of NIK mRNA level inhibition. Lanes 1; No Treatment, 2; Mock, 3; siRNA 1180, 4; siRNA 1269, 5; siRNA 1397. **B**, Suppression of NIK expression by siRNA 1397. Lanes 1; No Treatment; 2; Mock, 3; 250pM, 4; 12.5pM, 5; 0.625pM, 6; 0.0625pM. **C**, RT-PCR of decreased NIK expression pattern. Lanes 1; siRNA, 2; siRNA + lipofectamine™ 2000, 3; siRNA + DMTAP liposome, 4; siRNA + SG-DMTAP liposome, 5; serum-free medium, 6; DMTAP liposome, 7; SG-DMTAP liposome.

DMPAP liposomes as shown in Fig. 1D.

Suppression of NIK mRNA (RT-PCR)

According to the RT-PCR analysis, NIK mRNA expression was decreased by siRNAs 1180 and 1269 in HepG2 cells and by siRNAs 1180 and 1397 in HepG2.2.15 cells, respectively. As shown in Fig. 3A, the suppression of NIK mRNA expression levels by 1397 was more specific in HepG2.2.15 than in HepG2 cells. These results indicated that siRNA 1397 exerted a specific effect on liver cancer that was derived from HBV infection only. Fig. 3B shows that NIK mRNA levels in HepG2.2.15 cells were inhibited by siRNA 1397 treatment, but the suppression of NIK mRNA in HepG2 cells was not statistically significant. In HepG2.2.15 cells, outstanding suppression of NIK mRNA expression was observed with 250 pM of siRNA 1397 treatment. As shown in Fig. 3C, NIK mRNA expression was decreased to the greatest extent by the SG-DMTAP encapsulated siRNA compared with other liposomal formulations such as DMTAP or Lipofectamine™ 2000. These results indicated that the SG-DMTAP liposome exerted a specific effect on liver cancer derived from HBV infection via targeting to the ASGPR on the cells.

Detection of the HBsAg level (ELISA)

Fig. 4 shows the silencing effects of siRNA 1397 in various formulations on the expression level of HBsAg in HepG2.2.15 cells. The HBsAg expression level was

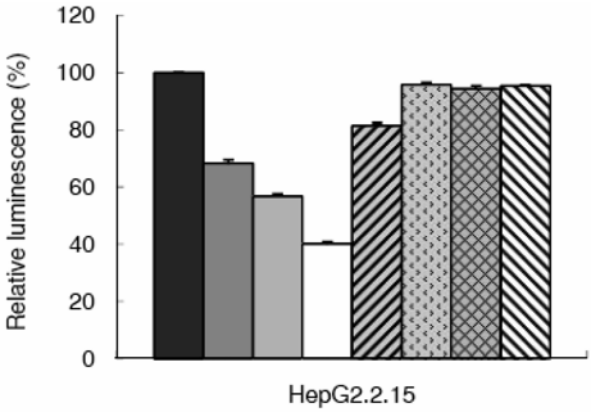

Fig. 4. Detection of the HBsAg level in HepG2.2.15 after treatment with siRNA 1397 in various formulations. ■ Control ■ siRNA+lipofectamine™ 2000 ■ siRNA + DMTAP □ siRNA +SG-DMTAP ▨ siRNA ▨ Lipofectamine™ 2000 only ▨ DMTAP only ▨ SG-DMTAP only.

inhibited by siRNA 1397 encapsulated in SG-DMTAP liposome by about 60% followed by DMTAP liposome and other formulations.

Stability of siRNA in liposomes

siRNA is easily degraded by RNase A (Fig. 5A). However, when encapsulated in liposomes, siRNA remained intact with time, though DSTAP liposome did not show a good protective effect after 30 min. The DSTAP liposome (Fig. 5E) was unable to protect siRNA from RNase A-mediated degradation for longer times than Lipofectamine™ 2000 (Fig. 5B), DOTAP (Fig. 5C) and DMTAP (Fig. 5D) liposomes. After 15 min, the siRNA encapsulated in DSTAP liposome was completely degraded by RNase A, however, the loaded siRNA in Lipofectamine™ 2000, DOTAP and DMTAP liposomes protected siRNA from RNase A after 1 h.

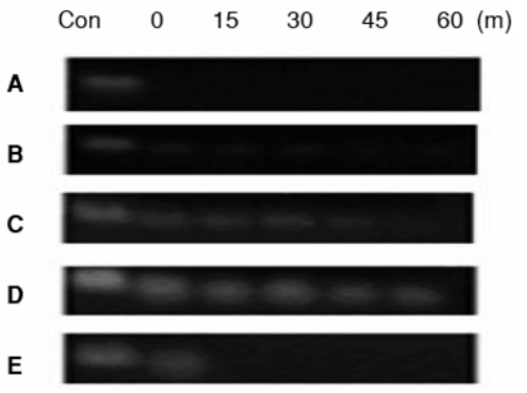

Fig. 5. Protection of siRNA from RNase A by liposomes. siRNA only **A**, siRNA in lipofectamine™ 2000 **B**, in DOTAP liposome **C**, in DMTAP liposome **D**, and in DSTAP liposome **E**.

Table I. Particle size and zeta potential of the siRNA-encapsulated DMTAP or SG-DMTAP liposomes

Liposome : siRNA	Zeta potential (mV)	Particle size (nm)
DMTAP : Cholesterol		
Liposome only	35.12 ± 1.58	102.6 ± 2.9
1:1 (molar ratio)	0.18 ± 0.14	144.2 ± 1.5
2:1	0.60 ± 0.32	199.0 ± 3.4
3:1	2.04 ± 0.84	210.4 ± 2.6
SG-DMTAP : Cholesterol		
Only	5.74 ± 1.10	136.6 ± 3.4
1:1	0.05 ± 0.02	168.6 ± 5.13
2:1	0.11 ± 0.34	236.7 ± 4.3
3:1	0.66 ± 1.11	278.2 ± 3.94

Characteristics of SG-DMTAP liposomes

Spherical SG-DMTAP liposomes were observed as shown in Fig. 6. The surface of the liposome was determined by zeta potential measurement (Table I). The zeta potential measurements indicated that DMTAP and SG-DMTAP liposomes possessed cationic charges. The charges of DMTAP and SG-DMTAP liposomes were 35.12 ± 1.58 mV and 5.74 ± 1.10 mV, respectively. SG-DMTAP liposome showed lower cationic zeta potential due to the addition of neutral SG. The incorporation of siRNA in DMTAP and SG-DMTAP liposomes resulted in a negative zeta potential in several combinations by changing the molar ratios. The molar ratio that caused the smallest particle sizes of DMTAP and SG-DMTAP liposomes with siRNA was 1:1 (liposome : siRNA). The particle size of the DMTAP liposome (102.6 ± 2.9 nm) was increased upon addition of SG (136.6 ± 3.4 nm). The encapsulation efficiency of siRNA into the SG-DMTAP liposome was about 36.73%.

The transfection efficiency of SG-DMTAP liposomes into HepG2.2.15 cells measured by GUAVA Express-Plus was about 82.83%. The fluorescence microscopy images captured 24 h post transduction with SG-DMTAP liposome demonstrated that fluorescence oligo encapsulated in the liposome was efficiently delivered to the target cells; thus the SG-DMTAP liposome is postulated to be an efficient vector in delivering therapeutic agents to HepG2.2.15 cells.

DISCUSSION

In general, the transfection efficiency of siRNA appeared to be higher than that of plasmid DNA regardless of the transfection method or cell lines. This is most likely due to the fact that plasmid DNA is larger and has to be delivered to the nucleus, whereas siRNA

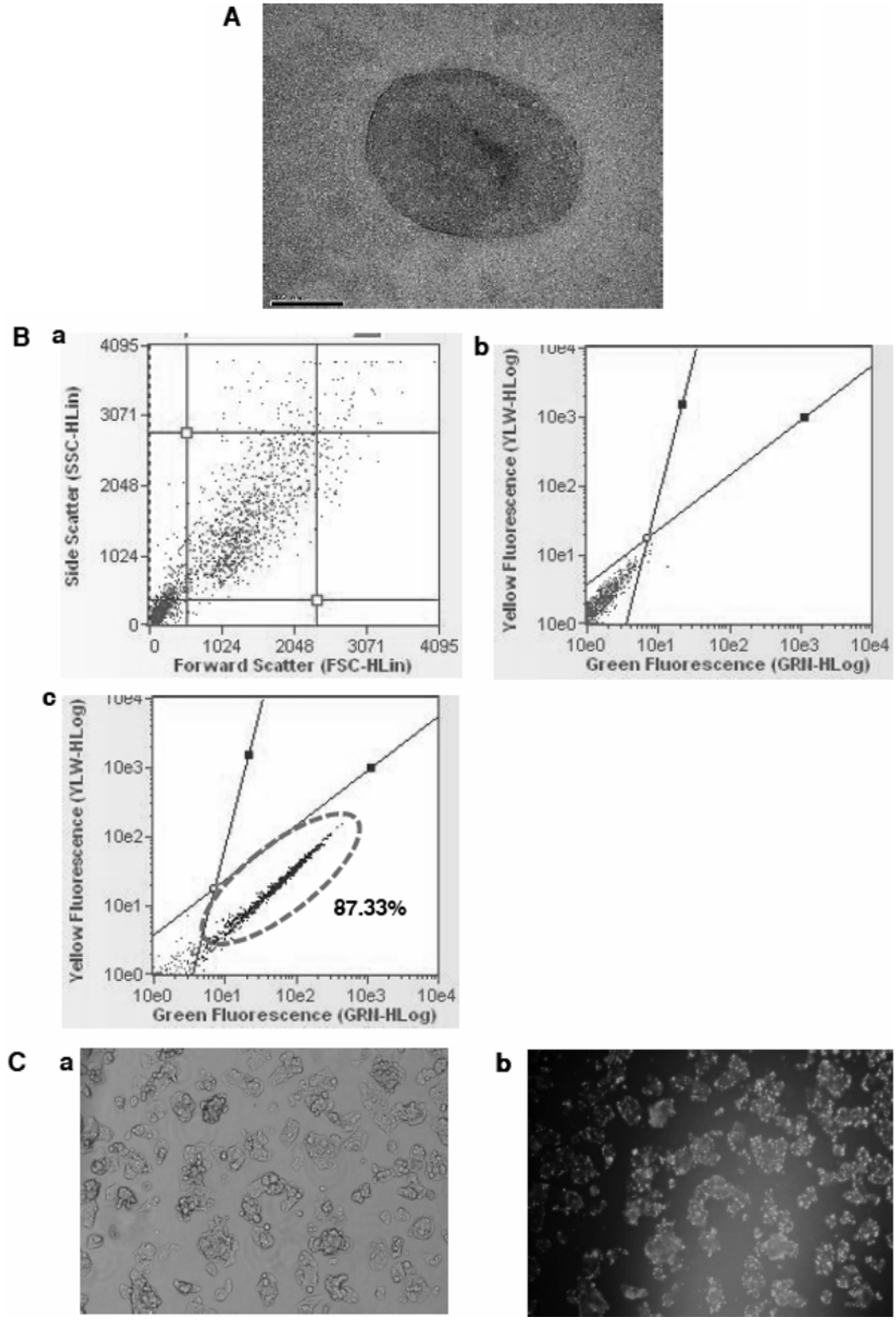

Fig. 6. A, Transmission Electron Micrograph of SG-DMTAP liposome; Lamella structure of SG-DMTAP liposome was observed. **B**, Transfection Efficiency Test through GUAVA ExpressPlus Assay; (**a**) Cell Distribution of HepG2.2.15 cells, (**b**) Fluorescence of HepG2.2.15 cells without fluorescence oligo transfection, **c**, Fluorescence of fluorescent oligo encapsulated in the SG-DMTAP liposome. **C**, Fluorescence microscopy analysis of HepG2.2.15 cells. (**a**) Microscopic image of the entire cells, (**b**) Fluorescence microscopic images of the transfected parts of cells; Fluorescence microscopy images were captured 24 h post-transduction with SG/DMTAP liposome (magnification × 10).

is relatively small and is active in the cytoplasm. Antisense and ribozyme approaches are available for some genes, but these approaches are not reliable enough for systemic gene silencing in cultured cells. In contrast, RNAi offers an effective and convenient means of assaying gene function in mammalian cancer cells.

In the present study, we showed that the activation of NIK was inhibited by RNAi-mediated degradation of target mRNA. siRNAs with specificity for NIK protein were designed and synthesized in an effort to reduce NIK expression. We evaluated the gene silencing effects of these siRNAs in suppressing NIK mRNA level in human liver cancer cells, HepG2 and HepG2.2.15, but not in human lung cancer cells, A549. HepG2.2.15 cells are derivatives of the HepG2 cells that have been stably transformed with several copies of the HBV genome.

Our results showed that proliferation of HBV-mediated HCC cells was reduced by NIK-specific siRNAs. To assess the therapeutic efficacy of NIK-specific siRNA, MTT and luciferase assays were used. All the designed siRNAs suppressed the expression level of NF-κB in all cells tested. These results indicated that the designed siRNAs effectively decreased NF-κB activity in all cells. Results from replicated RNA isolation and RT-PCR showed that hepatoma was induced by NF-κB activation. At the same time, it was confirmed that NF-κB was activated by NIK, which was expressed as a result of HBV-mediated stimulation among the three siRNAs tested. siRNA 1397 showed the highest inhibition of NIK expression. Taken together, all three siRNAs (1180, 1269 and 1397) efficiently inhibited NIK expression in HCC cells, while siRNA 1397 specifically inhibited HBV replication.

To develop siRNA as a therapeutic agent, its stability and efficiency and specific tissue-targeted delivery are required. Among the various types of non-viral vector systems, cationic liposomes seem to be the most promising because of their high gene expression efficiency. To gain stability and efficiency, DMTAP was used to prepare cationic liposomes, and SG was included to specifically deliver the liposome to liver cancer cells. In the present study, we also showed that DMTAP liposomes increased the stability and efficiency of siRNA.

We investigated the specificity of SG-DMTAP liposomes with siRNA by MTT and luciferase assays, RT-PCR analysis, and detection of HBsAg levels. These results demonstrated that DMTAP liposomes could be an effective vector for siRNA delivery. Treating HepG2.2.15 cells with siRNA encapsulated in SG-DMTAP liposome suppressed cell growth by about 60%. These results could be attributed to the specific hepatocyte-targeting behavior of SG. Moreover, SG-DMTPA liposomes showed high transfection efficiency (87.33%) when transfected into HepG2.2.15 cells. Therefore, this study established an efficient receptor-mediated delivery system for siRNA into hepatocytes using SG-containing DMTAP liposomes.

In conclusion, siRNA 1397 was shown to be capable of inhibiting HBV replication and DMTAP liposomes were found to stably and efficiently deliver this siRNA into the target cells. Moreover, SG improved the targeting ability of DMTAP liposomes specifically to hepatocytes. Thus, the siRNA 1397 encapsulated in SG-containing DMTAP liposome is expected to be a novel therapeutic entity for HBV-derived human HCC.

ACKNOWLEDGEMENTS

This study was supported by the Science Research Center (SRC) program of KOSEF (Research Center for Women's Diseases).

REFERENCES

Dykxhoorn, D. M., Novina, C. D., and Sharp, P. A., Killing the messenger: short RNAs that silence gene expression. *Nat. Rev. Mol. Cell Biol.*, 4, 457-467 (2003).

Elbashir, S. M., Harborth, J., Lendeckel, W., Yalcin, A., Weber, K., and Tuschl, T., Duplexes of 21-nucleotide RNAs mediate RNA interference in cultured mammalian cells. *Nature,* 411, 494-498 (2001).

Ghosh, S., and Karin, M., Missing pieces in the NF-kappaB puzzle. *Cell,* 109 Suppl, S81-96 (2002).

Hannon, G. J., RNA interference. *Nature*, 418, 244-251 (2002).

Kawano, K., Nakamura, K., Hayashi, K., Nagai, T., Takayama, K., and Maitani, Y., Liver targeting liposomes containing beta-sitosterol glucoside with regard to penetration-enhancing effect on HepG2 cells. *Biol. Pharm. Bull.,* 25, 766-770 (2002).

Kittler, R., and Buchholz, F., RNA interference: gene silencing in the fast lane. *Semin. Cancer Biol.,* 13, 259-265 (2003).

Malinin, N. L., Boldin, M. P., Kovalenko, A. V., and Wallach, D., MAP3K-related kinase involved in NF-kappaB induction by TNF, CD95 and IL-1. *Nature,* 385, 540-544 (1997).

Mann, D. A., and Oakley, F., NF-kappaB: a signal for cancer. *J. Hepatol.,* 42, 610-611 (2005).

Nakano, H., Shindo, M., Sakon, S., Nishinaka, S., Mihara, M., Yagita, H., and Okumura, K., Differential regulation of IkappaB kinase alpha and beta by two upstream kinases, NF-kappaB-inducing kinase and mitogen-activated protein kinase/ERK kinase kinase-1. *Proc. Natl. Acad.*

Sci. U. S. A., 95, 3537-3542 (1998).

Okamoto, T., Sakurada, S., Yang, J. P., and Merin, J. P., Regulation of NF-kappa B and disease control: identification of a novel serine kinase and thioredoxin as effectors for signal transduction pathway for NF-kappa B activation. *Curr. Top. Cell. Regul.,* 35, 149-161 (1997).

Qi, X. R., Yan, W. W., and Shi, J., Hepatocytes targeting of cationic liposomes modified with soybean sterylglucoside and polyethylene glycol. *World J. Gastroenterol,* 11, 4947-4952 (2005).

Rabe, C., Cheng, B., and Caselmann, W. H., Molecular mechanisms of hepatitis B virus-associated liver cancer. *Dig. Dis.,* 19, 279-287 (2001).

Richmond, A., Nf-kappa B, chemokine gene transcription and tumour growth. *Nat. Rev. Immunol.,* 2, 664-674 (2002).

Ryu, H. M., Park, S. G., Yea, S. S., Jang, W. H., Yang, Y. I., and Jung, G., Gene expression analysis of primary normal human hepatocytes infected with human hepatitis B virus. *World J. Gastroenterol,* 12, 4986-4995 (2006).

Sharp, P. A., RNA interference--2001. *Genes Dev.*, 15, 485-490 (2001).

Sorensen, D. R., Leirdal, M., and Sioud, M., Gene silencing by systemic delivery of synthetic siRNAs in adult mice. *J. Mol. Biol.,* 327, 761-766 (2003).

Stark, G. R., Kerr, I. M., Williams, B. R., Silverman, R. H., and Schreiber, R. D., How cells respond to interferons. *Annu. Rev. Biochem.,* 67, 227-264 (1998).

Zandi, E., Rothwarf, D. M., Delhase, M., Hayakawa, M., and Karin, M., The IkappaB kinase complex (IKK) contains two kinase subunits, IKKalpha and IKKbeta, necessary for IkappaB phosphorylation and NF-kappaB activation. *Cell,* 91, 243-252 (1997).

Zhang, Y., Rong Qi, X., Gao, Y., Wei, L., Maitani, Y., and Nagai, T., Mechanisms of co-modified liver-targeting liposomes as gene delivery carriers based on cellular uptake and antigens inhibition effect. *J. Control. Release.,* 117, 281-290 (2007).